# Mechanical coupling of microwave and optical photons

Vincent Baker, Drexel University Department of Physics

December 7, 2015

**Abstract**

Quantum electromagnetic phenomenon are of both theoretical and practical interest. Quantum phenomenon are more readily observable at high energies where individual photons are well localized. New methods of coherent coupling between optical and microwave systems hold the promise of extending quantum techniques into the microwave regime.

## 1 Introduction

Coupling between optical and microwave modes creates a new set of experimental techniques to explore the principles of quantum dynamics. The coherent transfer of quantum states may be exploited in applications including quantum-enhanced sensing and quantum computing. Several similar mechanisms for optical/microwave coupling have been reported recently [1, 3].
We will start by reviewing some of the proposed methods for microwave/optical coupling. We then sketch the analytical exploration of the nanomechanical resonator from [3] to demonstrate some important aspects of the approach. The application to quantum illumination, in particular quantum radar, is discussed in the final section.

## 2 Optical/Microwave Coupling Methods

Several methods for coupling optical and microwave systems have been investigated. In [3] the authors propose coupling microwave and optical cavity modes through a mechanical resonator. The resonator itself is a drum-head capacitor that is coupled to the microwave cavity through a planar spiral inductor. The equivalent electrical circuit is resonant at microwave frequencies. One surface of the mechanical resonator is coated with a mirrored finish and caps the end of an optical cavity. The optically-induced mechanical motion changes the capacitance of the microwave resonator circuit, providing the desired coupling.

In [1] the authors have experimentally characterized a coupled microwave/optical system using a beam of piezoelectric material (AlN) patterned as a photonic crystal suspended over a cavity (figure 2). The crystal is driven directly by a microwave signal injected directly onto the beam. The optical coupling is acheived by routing an optical waveguide to a separation of $< 1$ optical wavelength from the crystal. The crystal has a transverse mechanical resonance at 4GHz which is electrically excited. The optical coupling point (see figure 2) is placed at the mechanical resonance point, so that the electrically excited mechanical motion interacts with the optical transmission.
The authors in [1] experimentally examine the nature of the coupling between the optical and mechanical modes. The authors demonstrate the detuning of the optomechanical crystal via a an applied DC voltage (figure ). It is clear

Figure 1: Optical and microwave cavities entangled through a mechanical resonator. A, Proposed experimental setup. B, Equivalent circuit diagram of microwave resonator.

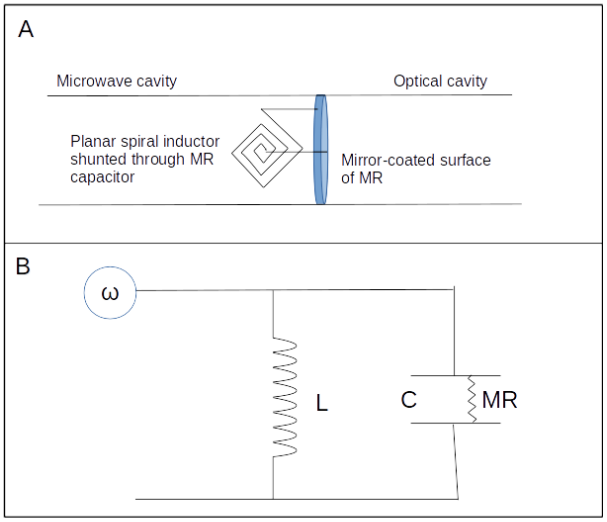


Figure 2: Optomechanical piezo crystal device from [1]. a. SEM image showing the optical couplers and waveguide (red), piezoelectric photonic crystal (blue) and microwave contacts (yellow). b. Close-up of the optical coupling point and numerical simulation of the optical and mechanical resonant modes.

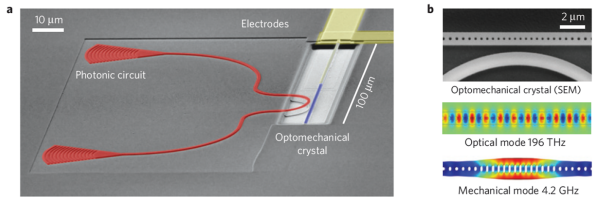


that, for sufficient microwave excitation and piezoelectric actuation, the microwave signal will influence the transmitted optical signal. The most obvious effect will be an amplitude modulation of the optical signal at the microwave excitation frequency. To acheive the desired optical/microwave correlation the couling must also carry the microwave phase into the optical signal.

Figure 3 shows the experimental setup using homodyne mixing of an optical signal that has been downcoverted through photodetection and low-pass filtering to isolate the optical sideband related to the mechanical resonance. The Argand diagram of the received signal for different phases of the injected microwave signal show that the microwave phase is retained in the coupled optical signal.

With both the amplitude and phase correlated the authors then demonstrate optical transparency controlled by the frequency and phase of the microwave signal. The primary optical carrier is detuned from the optical cavity resonance by the microwave frequency ($\omega_{drive} = \omega_o - \omega_w$). Optical sidebands are added to the signal and swept across the cavity resonance frequency. The sideband transmission can now be controlled entirely by the microwave signal (figure 4 ). The absorbtion peak width (200 Hz) is much narrower than the microwave resonance (1.7 Mhz).

The optomechanical piezoelectric crystal was fabricated as an integrated electronic/photonic device. This is a strongly supported area of engineering research, as exemplified by the new Integrated Photonics Institute for Manufacturing Innovation, an institute with almost 100 academic and industry members funded with $110M federal funding and over $500M cost share from the members [2]. As these engineering and manufacturing methods improve these types of nanomechanical systems will become readily available to physics researchers.

Figure 3: Top: Homodyne detection experiment from [1]. Bottom: Argand diagram showing homodyne detection of signal injected at different phases (red) as well as the noise with no microwave input (gray)

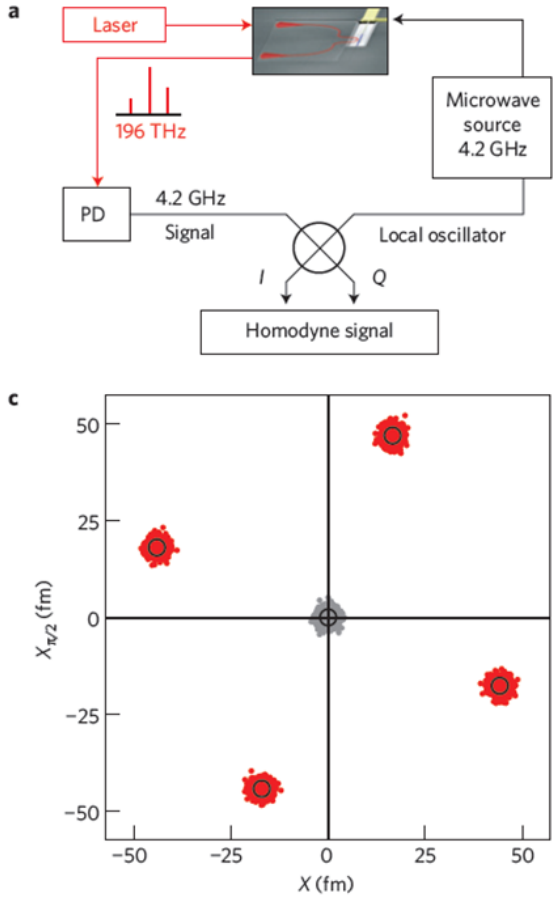


Figure 4: b. Optical sideband transmission across the resonance band for microwave detunings $2\pi\{-1, 0, 1\}$ Mhz. The blue and red traces are for microwave phase shifts $0, \pi$. c. Optical sideband transmission at optical detunings $\Delta = 2\pi\{-1, 0, 1\}$ MHz as the microwave source is swept across the resonance.[1].

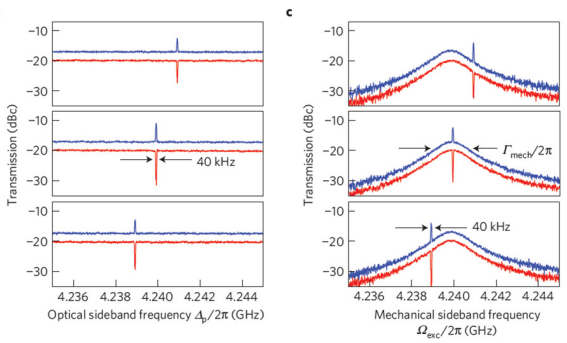


## 3 Analysis of the Mechanical Resonator Dynamics

We present the analysis of the nanomechanical resonator system in [3] to illustrate some of the relevant analytical methods. The Hamiltonian of the combined system is expressed in terms of the creation and annihilation operators of the optical and microwave cavities. The effects of thermal noise are incorporated through a set of quantum Langevin equations, which are then linearized about a stationary point. Finally the correlation matrix of the system is developed, from the which the logarithmic negativity can be calculated. The log-negativity is a measure of the degree of entanglement between the elements of the system, and the results demonstrate the entanglement between the optical and microwave modes.

We treat the nanomechanical resonator as a one-dimensional harmonic oscillator. We use the subscripts $w, m, c$ to denote parameters of the microwave cavity, mechanical resonator and optical cavity respectively. The cavities are driven at frequencies detuned from reso-

nance by $\Delta_{0w}$ and $\Delta 0c$. The Hamiltonian of the system shown in figure 1 is then:

$$\begin{aligned} H =& \frac{p_x^2}{2m} + \frac{m\omega_m^2 x^2}{2} \\ &+ \frac{\Phi^2}{2L} + \frac{Q^2}{2(C + C_0(x))} - e(t)Q \\ &+ \hbar\omega_c a^\dagger a - \hbar G_{0c} a^\dagger a x \\ &+ i\hbar E_c \left(a^\dagger e^{-i\omega_{0c}t} - a e^{i\omega_{0c}t}\right) \end{aligned} \tag{3.1}$$

Where $a^\dagger, a$ are the creation and annihilation operators of the optical cavity, $\Phi, Q$ are the flux through the inductor and the charge on the capacitor, $e(t) = -i\sqrt{2\hbar\omega_w L}E_w \left(e^{i\omega_{0w}t} - e^{-i\omega_{0w}t}\right)$ is the driving function of the microwave cavity and $G_{0c} = \frac{\omega_c}{L}\sqrt{\hbar/m\omega_m}$ gives the optomechanical coupling rate with resonator mass m and optical cavity length L, and $E_c = \sqrt{2P_c\kappa_c/\hbar\omega_{0c}}$ is the optical input.

The quadratic form of the microwave resonator circuit is amenable to expression in terms of microwave creation and annihilation operators $b, b^\dagger$. We can then work in the interaction picture with respect to:

$$H_0 = \hbar\omega_{0w} b^\dagger b + \hbar\omega_{0c} a^\dagger a \tag{3.2}$$

We can now express the time-dependent Hamiltonian in terms of the cavity detunings and neglect higher-order terms at $\pm 2\omega_{0w}, \pm 2 \pm \omega_{0c}$ since they will oscillate quickly and tend to average out. The final Hamiltonian is:

$$\begin{aligned} H =& \hbar\Delta_{0w} b^\dagger b + \hbar\Delta_{0c} a^\dagger a \\ &+ \frac{\hbar\omega_m}{2}(\hat{p}^2 + \hat{q}^2) - \hbar G_{0w}\hat{q} b^\dagger b - \hbar G_{0c}\hat{q} a^\dagger a \\ &+ i\hbar E_w (b^\dagger - b) + i\hbar E_c (a^\dagger - a) \end{aligned} \tag{3.3}$$

The fourth and fifth terms of the Hamiltonian are the coupling terms between the microwave and optical cavities and the mechanical resonator.

Figure 5: Mean number of thermal photons in the microwave cavity (top) and the optical cavity (bottom)

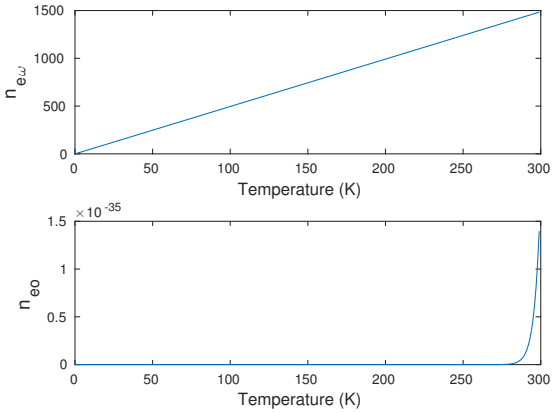


We also consider thermal effects for both systems. We plot the expected number of thermal photons for both the optical system (500 THz) and the microwave system (4.5 GHz) in Figure 5.

$$\langle n \rangle_e = \frac{1}{z^{-1}e^{\beta\hbar\omega} - 1} \tag{3.4}$$

We can clearly neglect thermal noise in the optical part of the system, but we must include noise terms in the microwave system even at low temperatures. To incorporate the noise terms the authors introduce a set of quantum Langevin equations (QLEs), differential equations for the time evolution of the system.

$$\dot{q} = \omega_m p \tag{3.5}$$

$$\dot{p} - -\omega_m q - \gamma_m p + G_{0c} a^\dagger a + G_{0w} b^\dagger b + \xi \tag{3.6}$$

$$\dot{a} = -(\kappa_c + i\Delta_{0c})a + iG_{0c} q a + E_c \tag{3.7}$$

$$\begin{aligned} \dot{b} =& -(\kappa_w + i\Delta_{0w})b + iG_{0w} q b + E_w \\ &+ \sqrt{2\kappa_w} b_{in} \end{aligned} \tag{3.8}$$

Where $\kappa_c, \kappa_w$ are the damping functions of the optical and microwave cavities, $\xi$ is the quantum Brownian noise acting on the mechanical

resonator, and $b_{in}$ is the noise function for the microwave input.

The authors then investigate the steady state of the driven system by setting the derivatives in the QLEs equal to 0. One question not addressed in this paper is the time for the system to reach steady state. This settling time will be important for quantum illumination systems that use pulsed signals that are not continuous in time. The authors write the steady-state parameter values as $q_s, p_s, a_s, b_s$ with corresponding fluctuations $\delta q, \delta p, \delta a, \delta b$. The equilibrium values are found by setting the derivatives to 0:

$$p_s = 0 \tag{3.9}$$

$$q_s = \frac{G_{0c}|a_s|^2 + G_{0w}|b_s|^2}{\omega_m} \tag{3.10}$$

$$a_s = \frac{E_c}{\kappa_c + i\Delta_c} \tag{3.11}$$

$$b_s = \frac{E_w}{\kappa_w + i\Delta_w} \tag{3.12}$$

Where we have written $\Delta_c = \Delta_{0c} - G_{0c}q_s$ and $\Delta_w = \Delta_{0w} - G_{0w}q_s$. These are the caivty detunings for the optical and microwave fields. Expanding about the equilibrium point:

$$\delta\dot{q} = \omega_m \delta p \tag{3.13}$$

$$\delta\dot{p} = -\omega_m\delta q - \gamma_m\delta p + G_{0c}a_s(\delta a^\dagger + \delta a) + G_{0w}b_s(\delta b^\dagger + \delta b) + \xi \tag{3.14}$$

$$\delta\dot{a} = -(\kappa_c + i\Delta_c)\delta a + iG_{0c}a_s\delta q + \sqrt{2\kappa_c}a_{in} \tag{3.15}$$

$$\delta\dot{b} = -(\kappa_w + i\Delta_w)\delta b + iG_{0w}b_s\delta q \tag{3.16}$$

Having obtained the dynamics of the fluctuations of the system about the equilibirum point, the authors now analyze the correlations between the three component systems.

## 4 Correlation analysis

There are several measures of entanglement in quantum information theory. A bipartite system is completely separable (unentangled) if it can be written as combinations of the tensor product of the component systems:

$$\rho^{ab} = \sum_i c_i \rho_i^a \otimes \rho_i^b \tag{4.1}$$

When $\rho^{ab}$ is a pure state the degree of entanglement can be determined from reduced density matrix with respect to one of the component systems:

$$\rho^a \equiv Tr_b(\rho^{ab}) \tag{4.2}$$

$$S = -Tr(\rho^a \ln \rho^a) \tag{4.3}$$

For mixed states the evaluation is more complicated. In [6] the authors introduce a computable entanglement metric for a bipartite mixed state, the negativity:

$$N(\rho) \equiv \frac{\|\rho^{T_a}\|_1}{2} \tag{4.4}$$

Where $\|\rho^{T_a}\|_1$ is the trace norm of the partial transpose of $\rho$ with respect to component system a. The authors in [3] use the logarithm of the negativity as their measure of entanglement. After extracting the correlation matrix of the fluctuations (eq 3.1-3.18) they compute the log-negativity of the three bipartite systems (optical-resonator, microwave-resonator, optical-microwave) shown in figure 6. The optical-microwave entanglement is the desired effect. There is substantial optical-microwave entanglement at low temperatures. One critical system parameter is the resonator mass: lower resonator mass increases the optical/microwave entanglement and reduces the optical/resonator entanglement.

## 5 Discussion of quantum radar

Quantum-enhanced sensing is a relatively young field that seeks to enhance sensing by using quantum entanglement. We discuss the particular application of quantum illumination

Figure 6: Log-negativity for the three bipartite systems (OC-MC black, OC-MR dashed red, MC-MR dashed blue) vs. normalized cavity detuning $\Delta_w/\omega_m$ at $T = 100mK$(a),$T = 200mK$(b) and $T = 250mK$(c)[3]

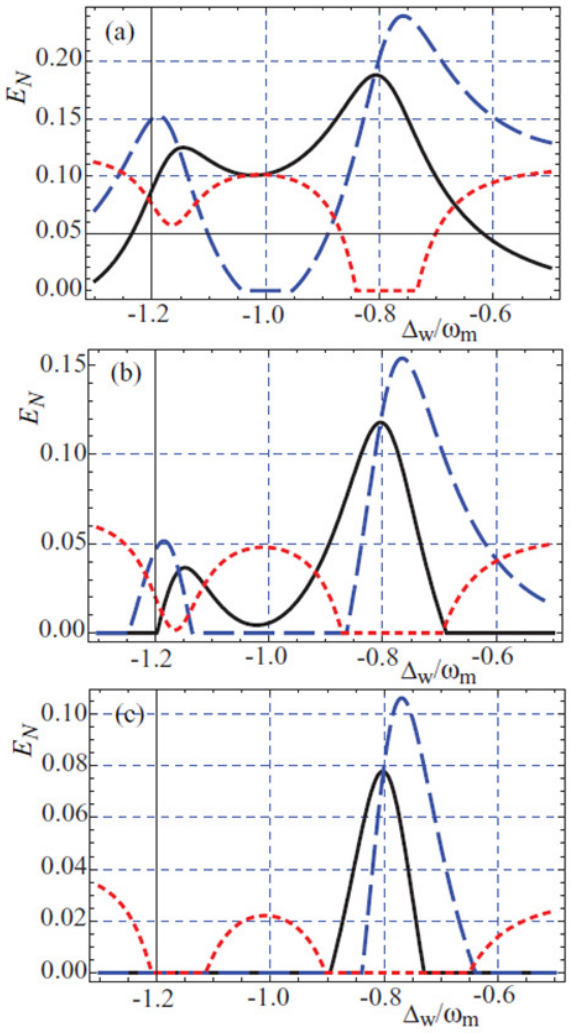


in the microwave regime applied to radar systems. Radar systems determine the range, bearing and velocity of an object by emitting a microwave signal and measuring the signal reflections. Radar waveforms are designed to allow the receiver to correlate the return signal from an object of interest in the presence of thermal noise, interfering signals and signal reflections from other objects. Quantum illumination can improve this correlation and can theoretically provide better performance than any conventional microwave system [4][5].

One key performance metric in the current quantum illumination literature is the probability of detecting a target. In [5] the authors consider illuminating a strong thermal bath (average photon number $N_\beta \gg 1$) with a weak optical illumination. They considered the thermal bath as a Gaussian state (previous work included only a microcanonical ensemble model of the thermal bath). The illuminator source is the output of a spontaneous parametric downconversion process, so that an entangled pair of photons is generated with $N_S$ the average number of photons per mode. One of the photons is retained as the idler photon with annihilation operator $\hat{a}_I$, one photon is used as the source photon with annihilation operator $\hat{a}_S$. When there is no target present the annihilation operator for the return signal is simply $\hat{a}_R = \hat{a}_B$. When there is a target present the return signal annihilation operator can be writting $\hat{a}_R = \sqrt{\kappa}\hat{a}_S + \sqrt{1-\kappa}\hat{a}_B$. With $\kappa \ll 1$ this represents a weak return signal.

The authors show that the Wigner-distribution covariance matrix when there is no target present $\Lambda^0$ and when a target is present $\Lambda^1$

are:

$$\Lambda^0 = \frac{1}{4}\begin{bmatrix} B & 0 & 0 & 0 \\ 0 & B & 0 & 0 \\ 0 & 0 & S & 0 \\ 0 & 0 & 0 & S \end{bmatrix} \tag{5.1}$$

$$\Lambda^1 = \frac{1}{4}\begin{bmatrix} A & 0 & \sqrt{\kappa}C_q & 0 \\ 0 & A & 0 & -\sqrt{\kappa}C_q \\ \sqrt{\kappa}C_q & 0 & S & 0 \\ 0 & -\sqrt{\kappa}C_q & 0 & S \end{bmatrix} \tag{5.2}$$

With $B = 2N_B{+}1$, $S = 2N_S{+}1$, $A \equiv 2\kappa N_S{+}B$ and $C_q \equiv 2\sqrt{N_S(N_S+1)}$ is a correlation term for the entangled system. The off-diagonal terms are greater

The authors then propose to measure the density matrix $\rho_{RI}$ of the idler and return signal. If both hypotheses are equally likely, the minimum error-probability decision rule is:

$$\rho^1_{RI} - \rho^0_{RI} > 0 \rightarrow H^1 \tag{5.3}$$

If $\{\gamma^+_n\}$ are the non-negative eigenvalues of $\rho^1_{RI} - \rho^0_{RI}$ then the error probability of the optimum quantum receiver is:

$$Pr(e) = \left(1 - \sum_n \gamma^+_n\right) \tag{5.4}$$

The authors are then able to develop Bhattacharrya bounds for the quantum illuminator and Chernoff bounds for a coherent-state classical illuminator, shown in 7. For a reasonable number of transmissions ($< 100$) the theoretical upper bound on the detection error probability is substantially lower than the theorectical lower bound on a coherent classical system. This result provides motivation for investigating quantum illumination.

In microwave quantum illumination the microwave probe photon will travel from the transmitter to the object to be detected, scatter from the object, and return to the detector. An optical photon, termed the idler photon,

Figure 7: Upper bounds on detection error probabilities for classical (solid blue) and quantum (solid red), with lower bound (dashed blue) for coherent classical systems. [5]

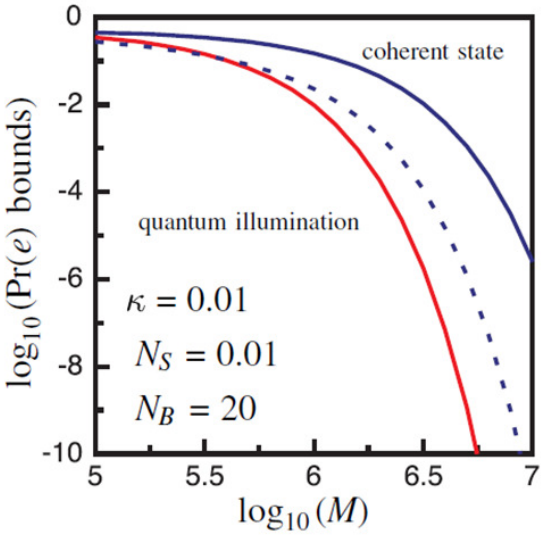


is initially entangled with the microwave photon (figure 8). The probe photons are not expected to remain in a coherent entangled state with the idler photons, yet there is a still an enhanced correlation between them even after decoherence [5].

As we have shown in figure 2 the optical quantum illumination is somewhat artifical as thermal effects are generally negligble at optical energies. The authors in [4] present microwave quantum illumination as a more realistic application of the same principles.

Even in the microwave regime the results in [5] and [4] are not necessarily relevant. Radar systems can employ very high-power microwave sources and highly directional antennas. Radar system performance is in general not limited by the thermal background noise but instead by "clutter": the scattered radar signals from objects not of interest. Typical clutter scatterers include ground, foliage, buildings, rain and

Figure 8: Proposed quantum radar system [4]

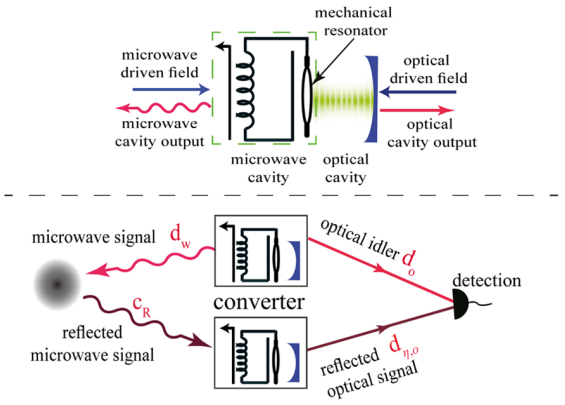


Figure 9: Passive (top) and active (bottom) phase arrays. In the active array, each element has a microwave source.

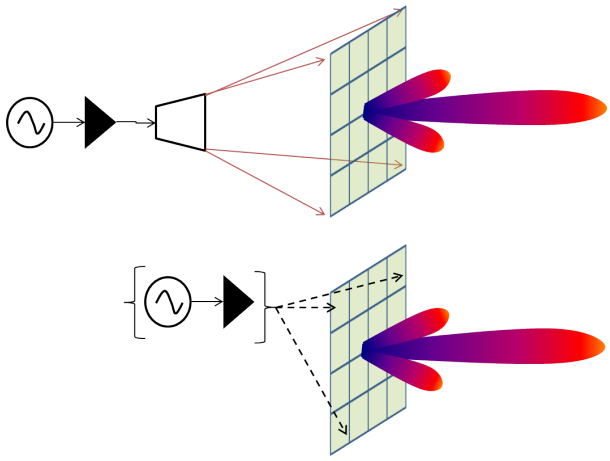


other atmospheric particulate. Moder radar systems mitigate clutter effects through the use of short signal pulses, directional antennas, and sophisticated waveforms. Any radar system employing quantum illumination must be able to employ similar techniques, or else the gains from quantum coherence will be more than offset by other losses.

Modern radar designs are dominated by the electronically steered array (ESA) antenna. An electronically steered antenna consists of many individual antenna elements, with each element able to individually control the phase shift of the transmitted and received signal. Two types of ESA are shown in figure 9. The passive ESA in the top figure has a single high-power microwave source, which illuminates a planar array of antenna elements. Each element in the array includes an electronically controlled phase shifter that changes the phase of the signal as it passes through. The lower figure shows an active ESA in which every antenna element includes a separate microwave source.

Applying quantum illumination to a phased array system will require the resolution of several questions. The schemes discussed so far may be compatible with a passive ESA. but it must be determined if passing the signal through many passive phase shifters will degrade the correlation with the idler signal. It is not alear how quantum illumination would be applied to an active ESA design. The active ESA signals are digitized at each individual element, and the antenna beamforming and signal correlation is done in the digital domain.

## References


[1] J. Bochmann A. Vainsencher D. Awschalom A. Cleland. "Nanomechanical coupling between microwave and optical photons". In: *Nature Physics* 9 (2013), pp. 712–716. DOI: 10.1038/NPHYS2748.

[2] *Integrated Photonics Institute for Manufacturing Innovation*. URL: http://manufacturing.gov/ip-imi.html.

[3] Sh. Barzanjeh D. Vitali P. Tombesi G.J. Milburn. "Entangling optical and microwave cavity modes by means of a nanomechanical resonator". In: *Annalen der Physik* 322.10 (1905), pp. 891–921. DOI: http://dx.doi.org/10.1002/andp.19053221004.

[4] Sh. Barzanjeh S. Guha C. Weedbrook D. Vitali J. Shapiro S. Pirandola. "Microwave quantum illumination". In: *Physical Review Letters* 114 (2015). DOI: http://dx.doi.org/10.1002/andp.19053221004.

[5] S. Tan B. Erkmen V. Giovannetti S. Guha S. Lloyd L. Maccone S. Pirandola J. Shapiro. "Quantum Illumination with Gaussian State". In: *Physical Review Letters* 101.253601 (2008). DOI: http://dx.doi.org/10.1103/PhysRevLett.101.253601.

[6] G. Vidal R.F. Wener. "Computable measure of entanglement". In: *Physical Review A* 65 (2002). DOI: http://dx.doi.org/10.1103/PhysRevA.65.032314.